Complete wetting transitions at the liquid-vapor interface of gallium-bismuth alloys: Single-wavelength and spectroscopic ellipsometry studies

S. Dogel, D. Nattland,* and W. Freyland
Institute of Physical Chemistry, Physical Chemistry of Condensed Matter, University of Karlsruhe, D-76131 Karlsruhe, Germany
(Received 8 April 2005; published 1 August 2005)

Complete wetting transitions at the liquid-vapor interface of Ga_xBi_{1-x} alloys (x_{Ga}=0.915, 0.88, 0.8, 0.67, and 0.57) have been investigated by ellipsometry. For this purpose we have developed a UHV apparatus equipped with an *in situ* phase modulation ellipsometer. The setup allows cleaning of the alloy surface under UHV conditions. Spectroscopic ellipsometry ($0.8\ \text{eV} \leqslant h\nu \leqslant 4.65\ \text{eV}$) at various constant temperatures and time-dependent measurements at a constant energy of 2.75 eV, while the sample was continuously cooled down, are utilized. These complementary approaches promise access to the functional form of the wetting film thickness with temperature as complete wetting is approached. A multistage analysis is introduced to extract the film thickness from single-wavelength ellipsometry. For a careful analysis of the spectra, it was necessary to reinvestigate the complex dielectric functions of the pure components bismuth and gallium. The spectra of the alloys have been modeled using an effective medium approximation for the liquid Ga-Bi bulk phase covered by a film of liquid bismuth. In our particular sample geometry, the wetting film thickness grows from one or two atomic layers to about 30 Å to 50 Å within a few K as one approaches the demixing regime. The data show the proposed logarithmic divergence of d, typical for short range interactions. In the temperature and composition range studied they do not agree with the functional form proposed for long range intermolecular interactions.

DOI: 10.1103/PhysRevB.72.085403 PACS number(s): 61.30.Hn, 61.25.Mv, 68.05.−n, 78.20.−e

I. INTRODUCTION

Research in the field of surfaces and interfaces, although possessing a long and successful tradition in chemistry and physics, is currently especially motivated by the interest in mesoscopic or nanoscaled systems, whose thermodynamic properties are strongly governed by the contribution of their interfaces. In this respect interfacial phase transitions, in general, and wetting transitions, in particular, which are still challenging for both experimentalists and theoreticians, are of profound relevance. A number of reviews can be looked up for a general survey of the field of wetting transitions.[1–3]

In the focus of the present study are binary fluid Ga-based alloys. First strong indications for the occurrence of wetting transitions in metallic systems were obtained by ellipsometry for Ga-Bi[4] and for Ga-Pb[5] employing Auger electron spectroscopy. The phase diagram of Ga-Bi[6,7] is sketched in Fig. 1. Both systems exhibit a demixing gap and the respective Ga-rich phase has the lower density and the higher surface tension.[8–10] To reduce the free energy of the system, a gravitationally thinned film of the Bi-rich (Pb-rich) phase completely wets spontaneously the Ga-rich bulk phase. On account of the ellipsometric measurements, the film thickness in Ga-Bi was roughly estimated as 50 Å. Recent x-ray reflectivity experiments are in good agreement with these results.[11,12]

Metallic systems are dominated by Coulomb interactions, which are exponentially screened and therefore short ranged. In this case theory predicts a logarithmic divergence of the wetting film thickness as complete wetting is approached from off coexistence. This was shown by Chatain and Wynblatt for Ga-Pb approaching the monotectic point along the solid (Pb)-liquid (Ga-rich) phase line.[5] Dietrich and Schick suggested that complete wetting in these systems is pinned to this tetra point of four phase coexistence (Pb solid, Pb-rich liquid, Ga-rich liquid, vapor).[13] The determination of the wetting film thickness d approaching the liquid-liquid demixing gap from off coexistence in $Ga_{0.88}Bi_{0.12}$ using x-ray reflectivity revealed also a dependence in agreement with $d = \xi \ln(\Phi/\Delta\mu)$.[11,12] Here, ξ is the bulk correlation length, Φ is a measure for the effective surface potential, and $\Delta\mu$ is the distance to coexistence.

The objective of this study is a systematic investigation of the wetting characteristics of Ga-Bi in the range of the demixing gap. The compositions covered are situated on both sides of the critical point. They are indicated in Fig. 1. We employ spectroscopic and single-wavelength ellipsometry to measure the real and imaginary part of the complex dielectric function $\varepsilon(h\nu) = \varepsilon_1(h\nu) - i\varepsilon_2(h\nu)$ of the sample as well as the thickness of the wetting film. The ellipsometer is firmly attached to an UHV apparatus in which the final step of sample cleaning can be performed. For the interpretation of the alloy spectra it was necessary to study the spectra of the pure components under the same experimental conditions. It is an advantage for the aim of the present study that the spectra of pure Ga and pure Bi are rather different and, consequently, offer a strong contrast.

II. EXPERIMENT

A. Experimental setup

According to the objectives outlined above, the experimental task is to study the thickness and the spectroscopic properties of wetting films at the liquid-vapor interface of gallium-bismuth alloys. Any surface study, in particular of

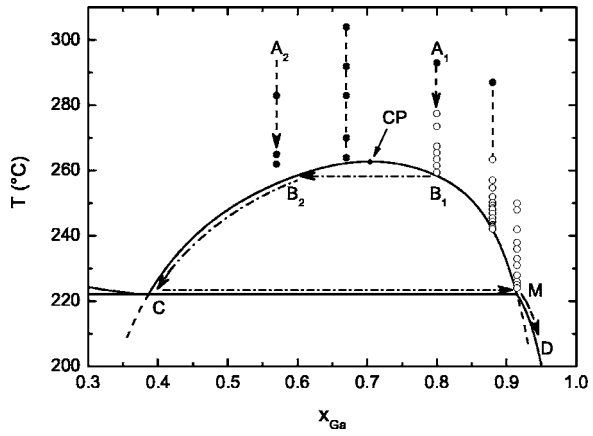

FIG. 1. High temperature Ga-rich part of the Ga-Bi phase diagram (solid lines) (Refs. 6 and 7). Vertical dashed lines show the experimental paths of time-dependent and spectroscopic experiments. Full circles present measurements where no wetting film was detected, open circles present measurements where a wetting film has formed. CP is the critical point at $x_{Ga,c}=0.7$ and $T_c=263$ °C. Dashed-dotted lines describe interfacial passages for two kinetic measurements described in Figs. 7 and 8 along the paths $A_1B_1B_2CMD$ for $x_{Ga}>x_{Ga,c}$ and A_2B_2CMD for $x_{Ga}<x_{Ga,c}$, respectively.

liquid metals, requires ultrahigh vacuum conditions (10^{-9} mbar and better) to obtain access to the free metal surface without oxides and other impurities. These requirements together with the necessary flatness of the liquid metal surface are major constrains for the design of our experimental setup.

This is shown in Fig. 2. It utilizes a phase modulation ellipsometer (UVISEL, Jobin Yvon) and a homemade stainless-steel UHV chamber. The pumping system consisting of a rotary vane pump, a turbo-pump, and an ion pump together with a liquid nitrogen trap allows achieving and maintaining a vacuum of nearly 10^{-10} mbar after sufficient bakeout. The entire setup is installed on a passive vibration insulating system of four air-pillows ④ to damp most vibrations, which are always present in a laboratory. It was found that such a simple system is sufficient for ellipsometric applications. The height of the sample ⑤ and the tilt of the chamber in respect to the liquid surface could be adjusted to fulfill the reflection conditions with the help of the linear driver ② and micrometer screws ③, respectively. To obtain atomically clean liquid surfaces, the setup is equipped with an argon sputtergun ⑥ and a homemade mechanical tungsten wire-cleaning device ⑦. Details of alignment and cleaning of the liquid alloy surface will be described below.

The modulator ⑧ and analyzer ⑨ heads of the ellipsometer are mounted on two inclined (~70°) flanges. A high stability Xe lamp is connected to the analyzer head with an optical fiber. Its light is linearly polarized and enters the chamber through a low strain UHV window. Vacuum tightness of that window is achieved by squeezing an In-wire ring. The beam (~Ø3 mm) is reflected from the liquid metal surface and reaches the modulator head through the second window. The phase of the signal is modulated by an oscillating (50 kHz) fused silica bar and passes a second polarizer.

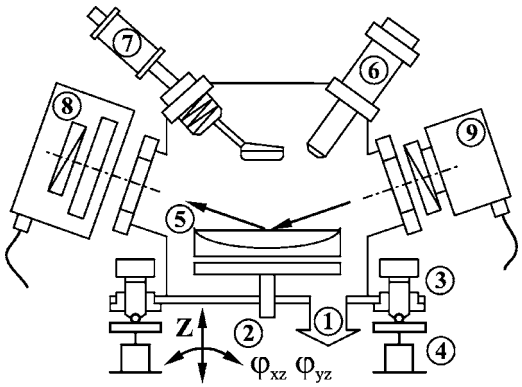

FIG. 2. Experimental setup of the phase modulation ellipsometer (UVISEL, Jobin Yvon) connected to the homemade UHV chamber: ①, pumping system, turbo and ion pumps (10^{-9} mbar); ②, sample height adjustment along z axis; ③, micrometer screws to tilt the whole apparatus in the xz and yz planes; ④, vibration damping system; ⑤, Mo crucible with the liquid alloy on the heater; ⑥, Ar sputter gun; ⑦, wobble stick and mechanical cleaning device; ⑧ and ⑨, modulator and analyzer heads of the ellipsometer.

The intensity after the monochromator is measured by a high sensitivity photo multiplier tube (PMT) for the ultraviolet-visible (UV-VIS) range and an InGaAs photodiode for near infrared (NIR). From the modulated signals the complex reflection ratio can be obtained, $\rho=\tan\Psi e^{i\Delta}$. It depends on the amplitude ratio $\tan\Psi$ and the phase shift Δ occurring upon reflection at the interface.[14] In this work the two intensities I_S and I_C were measured. For our particular settings of polarizer, modulator and analyzer they are connected to Ψ and Δ in the following ways: $I_S=\sin 2\Psi \sin\Delta$ and $I_C=\cos 2\Psi$.[15,16]

After the assembly of all components at the chamber, the precise angle of incidence Θ was determined by fitting the film thickness d and Θ to the well-known spectrum of an aged silicon wafer covered with a SiO_2 film. All data presented in this paper are based on a fixed angle of incidence of $\Theta=71.15°\pm0.05°$. The absolute accuracy of the ellipsometer is specified for Ψ and Δ with 0.1°. Recording several spectra under constant conditions, we obtained a reproducibility of 0.05° for both Ψ and Δ in almost the entire energy range. At the high and low energy ends of the spectra this error can be a little bit higher (~0.08°). A long time drift of Ψ and Δ at a fixed energy of 2.75 eV was found to be around 0.15°.

B. Crucible and sample preparation

Pure liquid Ga and Bi have high surface tensions[17] and strive for a curved free surface if the sample size is small. This is not suitable for any optical reflectivity study, since the light beam diverges after the reflection and the angle of incidence is not well defined. To avoid this disadvantage and reduce the total amount of high purity metals, a Mo crucible with a hemispherical cavity has been used.[8] If the crucible/sample interface is perfectly clean, the alloy wets the molybdenum and forms a flat sample/vacuum interface. The Mo crucible, which is inert for both components in the full temperature range of this study, was polished mechanically, then rinsed with acetone and ethanol and finally heated up to

1100 °C under vacuum better than 10^{-5} mbar. After this thermal treatment, the crucible was transported under vacuum into a glovebox (M. Braun, O_2, H_2O less than 1 ppm).

Even though the purity with respect to metallic impurities was given for Ga with 7 nines and for Bi with 5 nines there was always some nonmetallic slag visible on the surface. For purification the metals have been melted in a syringe. After flowing out of the tip of the syringe the nonmetallic impurities stuck to the wall. After this procedure both metals were always stored in solid state in the glovebox. For sample preparations the respective amounts of both metals (20–30 g of Ga, 6–20 g of Bi) were transferred in the crucible. The weighing accuracy was better than 1 mg, which leads to a negligible error of the mole fraction. The sample was solidified and quickly transported (in air) into the UHV chamber. It was placed on a cooling plate to ensure that the alloy remains solid during the following 15 h bakeout procedure. After a vacuum of about 10^{-8} mbar was achieved, the sample was shifted onto the heating element ⑤ using a linear driver. To homogenize the sample it was heated up with a resistance furnace to 250–300 °C for several hours. The temperature was measured with a NiCr-Ni (Type K) thermocouple inserted into the bottom of the crucible. The vertical and radial temperature gradients were estimated previously to be below 1 K at the temperatures of interest.[4] The temperature was controlled using a conventional (PID)-controller. The long term temperature stability was better than ±0.5 K. The thermocouple was calibrated at the melting point of pure Bi. The absolute accuracy was also better than ±0.5 K.

In spite of all precautions the liquid surface was covered with a thin but clearly visible layer of some impurities, presumably oxides. In this stage of the experiment, the sample did not wet the crucible. The alloy was sputtered for about half an hour using the Ar-ion source ⑥, which is very efficient as long as the oxide film covers the entire liquid surface. But after a certain time (~20 min) the film breaks into islands, which can float freely on the clean mirrorlike metal surface. Then the sputtering becomes ineffective since the oxide pieces evade the ion beam. For further cleaning we use a wire cleaner ⑦ similar to that described by Indlekofer *et al.*[18] It consists of a heatable tungsten wire (Ø0.5 mm, length 10 mm) fixed to a wobble stick, which allows it to move the wire along the entire surface of the liquid sample. The wire is brought into contact with the oxides, they stick to it and can be removed from the metal surface. For good sticking, the wire was heated to about 400 °C. The wire is then cleaned inside a protective container by heating it up to about 1200 °C for several seconds. Sputtering and wire cleaning have to be repeated several times until the surface is perfectly clean. Another important aspect is that now the liquid sample wets the crucible, which leads to a perfectly flat surface ideal for ellipsometry. After such a procedure no re-formation of oxide films was noticed for weeks as long as the vacuum conditions of 10^{-9} mbar were maintained. During sputtering and particularly during evaporation of the impurities from the wire cleaner, the windows of the chamber were shielded using magnetically driven metal screens. After sputtering and mechanical cleaning of the liquid surface, a small but unknown amount of alloy material was removed. However, a shift of the sample composition was not observed. This was seen from the cooling curves.

III. RESULTS

In this section we present the results of spectroscopic and time-dependent (kinetic) single-wavelength ellipsometric measurements at the vacuum-liquid alloy interface. The spectra have been evaluated either using a two-phase model or in the case of the presence of a wetting film, a three-phase model. Within the framework of the first, the optical properties—real and imaginary part of the dielectric function—can be directly calculated from the ellipsometric angles Ψ and Δ or, equivalently, from the quantities I_S and I_C. The latter model comprises the Ga-rich bulk phase, pure liquid Bi as the wetting film phase, and the vapor as ambient phase (see Ref. 14, p. 283). The angles Ψ and Δ in this model depend on the optical properties of the bulk phase and the film phase as well as on the film thickness d, which is here the quantity of interest. The film thickness can only be evaluated unambiguously when the spectra of the bulk phase and film phase are known with sufficient accuracy. This requires a good knowledge of the spectra of the pure components as well as of the homogenous alloys. For the spectroscopic characterization of the homogenous alloy phase, we employed the Bruggeman effective medium approximation (EMA),[19] which was developed to describe composite materials. Within this formalism the spectrum of the alloy can be calculated using the spectra of the pure components as input, weighed with the volume fraction. The procedure works surprisingly well for Ga-Bi alloys. This was verified by calculating the mole fraction of the alloy from the spectra. The agreement was within 0.01 units on the mole fraction scale.

A. Pure liquid Ga and Bi

The ellipsometric data in the whole spectroscopic range have been evaluated using the standard two-phase model: substrate and vacuum. The optical properties expressed, e.g., as the real and imaginary part of the dielectric function can be obtained directly from the primary ellipsometric intensities I_S and I_C. For each temperature, several spectra were recorded and averaged. In Fig. 3 the spectrum of liquid Ga at 256 °C is shown together with spectra available in the literature.[20,21] Both measurements deviate slightly from our spectra but outside the error limits. The data of Ref. 20 have been obtained at 850 °C and a shift of ε_1 and ε_2 is expected on account of the lower electron density and the lower conductivity. The origin of the deviations to Ref. 21 is not quite clear. However, Teshev and Shebzukhov do not give a precise description of their experimental conditions as far as the purity of the metals, the quality of the vacuum, and the cleanness of the surface is concerned. In Fig. 4 the spectra of liquid Bi at 298 °C is shown in comparison to published data.[20,22,23] The agreement is satisfactory within the error limits. Spectra at other temperatures are deposited as supplementary material.[24] In all further calculations we used our spectra as input data.

We have analyzed the spectra of the pure liquid components within the simple Drude free-electron model to extract

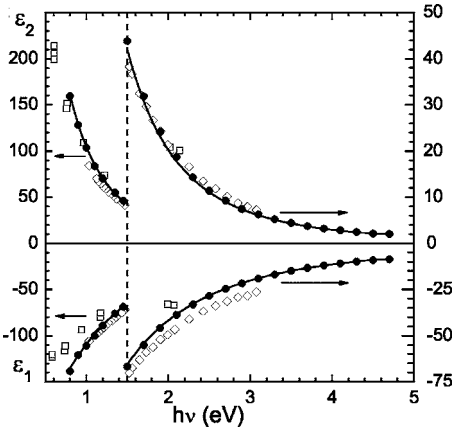

FIG. 3. Real and imaginary parts of the dielectric function for pure liquid Ga: ●, this work at 256 °C [see also Table I(a)]; solid lines, free-electron Drude fit to ●; ◇, 250 °C (Ref. 21); □, 850 °C (Ref. 20).

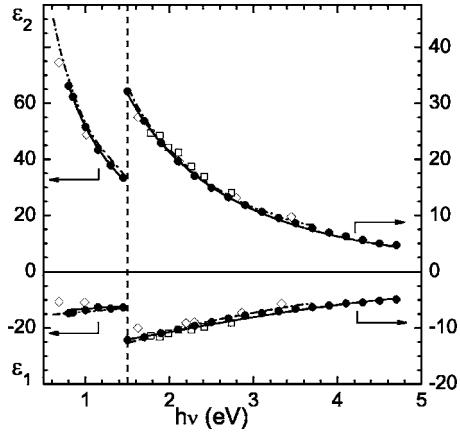

FIG. 4. Real and imaginary parts of the dielectric function for pure liquid Bi: ●, this work at 289 °C [see also Table I(b)]; solid lines, free-electron Drude fit to ●; dashed-dotted line, 285 °C (Ref. 23); ◇, 390 °C (Ref. 22); and □, 500 °C (Ref. 20).

parameters such as the plasma frequency ω_P and the damping frequency γ_D of the free electrons.[25] ω_P is proportional to the square root of the number density of the free electrons, which can be related to the mass densities of the metals[26] assuming three valence electrons for Ga and five for Bi. γ_D is closely related to the electronic mobility and the dc conductivity σ_0. It can be compared to direct measurements of the resistivity of the metals.[27] The best fit values of N_e and σ_0 at various temperatures are shown in Table I(a) for Ga and Table I(b) for Bi. The agreement between the values extracted from the spectra using the simple model and those obtained from direct measurements lies within 1.5% to 6%.

B. Ga-Bi alloys

The interfacial and wetting properties of liquid Ga-Bi alloys have been probed at constant overall composition approaching the coexistence line on cooling. We have recorded on the one hand various ellipsometric spectra at constant temperature for several compositions in the liquid-liquid demixing range (x_{Ga}=0.915, 0.88, 0.8, 0.67, and 0.57). On the other hand, we have measured the ellipsometric angles at a constant energy of 2.75 eV as a function of time as the sample was cooled down slowly.

The upper part of Fig. 5 shows the initial ellipsometric data in terms of I_S spectrum and I_C spectrum obtained at 293 °C for $Ga_{0.88}Bi_{0.12}$. At this temperature the alloy can be treated as a homogeneous mixture of both components. However, on account of the lower surface tension of liquid Bi in comparison to Ga there is always a thin microscopic layer of Bi adsorbed at the interface—see a model calculation[28] of the surface phase diagram of Ga-Bi. Even under the good conditions, in our experiment, it is difficult to resolve a monolayer employing ellipsometry at a liquid surface. Hence, the two-phase model is used to describe the spectra within an effective medium approximation. Using our spectra of the pure components the volume fraction of Ga, f_{Ga}, is the only parameter that can be easily converted to the mole fraction x_{Ga}. From the fit we obtain a composition of $x_{Ga}=0.88\pm0.01$, which coincides nicely with the weighted mole fraction. The same good agreement was observed for all data points drawn with full circles in the phase diagram (Fig. 1). This gave us some confidence for the applicability of the Bruggeman EMA for the description of the spectra of liquid Ga-Bi alloys. Moreover, in the case of the presence of a wetting film—i.e., a liquid Bi layer on top of a Ga-rich bulk phase—the correspondent three-phase fit to the spectra self-consistently approached the correct composition of the bulk phase when film thickness and composition was set as fitting parameters. In a second run the composition was fixed and the film thickness was the only parameter to be determined.

The middle panel and the lower panel of Fig. 5 show the development of I_S spectrum and I_C spectrum as the liquid-liquid coexistence is approached. To make the changes visible we plotted $I_S(T)-I_S(293\ °C)$ and $I_C(T)-I_C(293\ °C)$. It is particularly interesting to see the strong change in I_C and I_S in the small temperature interval from 248 °C to 242 °C. The solid lines represent three phase model fits to the spectra, which describe the experimental data at temperatures of 257 °C and 248 °C well within the experimental error. In close vicinity to liquid-liquid coexistence at 242 °C, the fit quality becomes clearly worse. As one approaches the complete wetting state at liquid-liquid coexistence, the three-phase model comprising a homogeneous liquid Bi film in contact with a homogeneous liquid Ga-Bi alloy seems to be a suboptimal description for the system. So far, the reason for this is not clear. Probably a diffuse or rough boundary between substrate and film could account for this discrepancy. This was suggested from x-ray reflectivity results.[11,12] However, since the deviations between experimental data and fit are still small (less than 2% in terms of I_C and I_S) the three-phase formalism was applied to all spectra to obtain a consistent description of the wetting film thickness in the temperature range studied. The thickness of the wetting films obtained in this way are shown in Fig. 6 as a function of the temperature distance from liquid-liquid coexistence, $\Delta T=T-T_{coex}$. At each temperature the system was equilibrated for 2 to 4 h. Three to five spectra were recorded and evaluated using the three-phase model.

TABLE I. (a) Pure liquid Ga. Sample temperature T, chamber pressure P_0, and the results of the fits of the Drude free-electron model to the ellipsometric spectra: ω_p and γ_D are the plasma and the damping frequency, N_e is the density of free electrons, σ_0 is the electronic dc conductivity. The errors of ω_p and γ_D are less than 2%. Comparison to direct measurements of density and conductivity is given in the last two columns. (b) Pure liquid Bi. Same notation as in (a).

		(a) This Work from Fits to the Spectra				Direct measurements	
						Ref. 26	Ref. 27
T (°C)	P_0 (10^{-9} mbar)	ω_p (eV)	γ_D (eV)	N_e (10^{23} cm^{-3})	σ_0 (10^4 Ω^{-1} cm^{-1})	N_e (10^{23} cm^{-3})	σ_0 (10^4 Ω^{-1} cm^{-1})
70	1.1	14.62	0.829	1.551	3.564	1.574	3.75
130	1.2	14.60	0.833	1.547	3.447	1.565	3.592
173	1.4	14.59	0.859	1.544	3.333	1.560	3.494
215	2.1	14.53	0.886	1.533	3.208	1.553	3.391
256	2.3	14.51	0.908	1.527	3.112	1.547	3.301
				(b)			
289	2.6	14.49	3.85	1.523	7.335	1.444	7.603
296	3.8	14.47	3.85	1.518	7.315	1.443	7.580
312	5.9	14.45	3.87	1.514	7.276	1.440	7.528
335	9.0	14.43	3.895	1.510	7.191	1.437	7.458
352	11	14.46	3.95	1.516	7.120	1.433	7.395
378	30	14.51	4.01	1.527	7.080	1.429	7.318

At large values of ΔT different starting thicknesses between 3 and 8 Å are obtained for different Bi compositions. The reason for this is not fully understood, but we have to mention that a film thickness of 3 Å is at the resolution limit of our experimental setup. Probably a slight change in the alignment of the ellipsometer with respect to the liquid surface accounts for this effect. An improved surface cleaning strategy after the first experiment at $x_{Ga}=0.915$ and a different spectral range could be other reasons. Nevertheless, all these experiments show a strong increase of the wetting film thickness as $\Delta T=0$ is approached. In particular the measurement at $x_{Ga}=0.915$ shows an important experimental observation: there is no detectable change of the liquid alloy surface over a long time period in our vacuum chamber. Different symbols (□, ◇) in Fig. 6 represent two runs separated by several days. A comparison of all three experiments can also help to get an insight in the maximum of the absolute experimental uncertainty of this study. It is estimated to be of the order of about one to two Bi layers. The error bars in Fig. 6 show the relative uncertainty of d at constant conditions of the alignment of the ellipsometer.

IV. DISCUSSION

The discussion of our results focuses on three main topics. First, we analyze qualitatively the ellipsometric results obtained at a selected wavelength on slow cooling from the homogeneous phase region above the critical point down to a temperature below the monotectic point. Second, we describe the strategy to extract the functional form of the film thickness of the wetting film as the liquid-liquid coexistence range is approached. In the last section we discuss the evolution of the film thickness obtained from the single-wavelength cooling curves as well as from ellipsometric spectra as a function of the chemical potential distance, $\Delta\mu$, to bulk liquid-liquid coexistence.

A. Analysis of cooling curves

Exemplarily for the temperature dependence of the ellipsometric parameters Ψ and Δ measured for various mole fractions in the composition range between $0.57 \leqslant x_{Ga} \leqslant 0.88$ we present here the results for $x_{Ga}=0.80$ in Fig. 7 and for $x_{Ga}=0.57$ in Fig. 8. As can be seen from the phase diagram in Fig. 1 the former sample is located on the Ga-rich side of the critical point and the latter on the Bi-rich side. The starting points of both experiments are indicated with arrows at A_1 and A_2 in Fig. 1. The upper part of Fig. 7 shows the temperatures of the furnace and the sample as a function of time. The furnace was cooled down slowly with a cooling rate of 3 K/h. The time intervals indicated at the top of the figure with roman numerals are related to different thermodynamic states and phase regions. Range I indicates the homogeneous region above the liquid-liquid miscibility gap, II is in the demixing gap, III corresponds to the monotectic reaction, and IV lies in the two-phase region where a Ga-rich liquid coexists with solid Bi. In the lower part of Fig. 7 the variations of the ellipsometric parameters Ψ and Δ with time are shown.

In our context here, case I (or phase region I) is of special interest: Ψ and Δ decrease continuously and accelerate as the demixing gap is approached. In this temperature range the

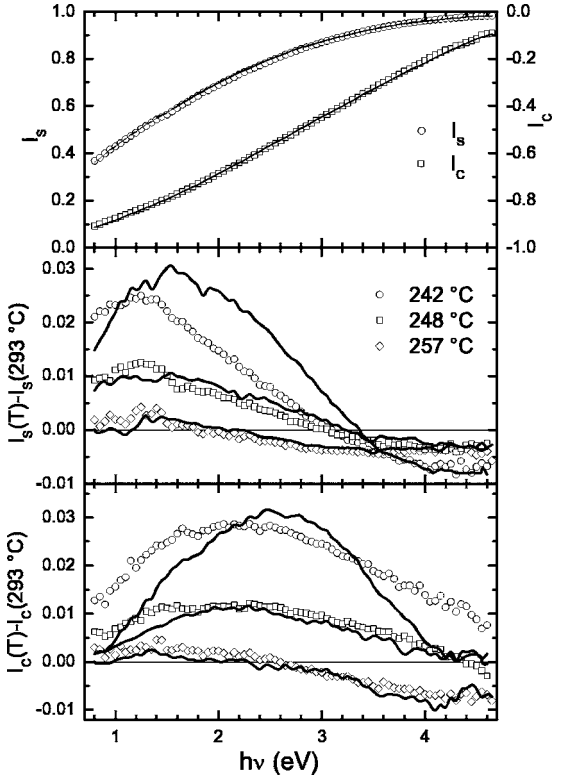

FIG. 5. Primary experimental data—intensities I_S and I_C. Upper section: I_S and I_C measured at 293 °C for a $Ga_{0.88}Bi_{0.12}$ alloy; solid lines show the fit within the framework of the two-phase model with an EMA used as substrate. Middle section: Variation of I_S at temperatures approaching the liquid-liquid coexistence line shown as difference relative to I_S (293 °C) to magnify the effect with temperature; solid lines present the three-phase model fits with EMA for the Ga-rich alloy as substrate and pure liquid Bi as film. Lower section: Same presentation for I_C.

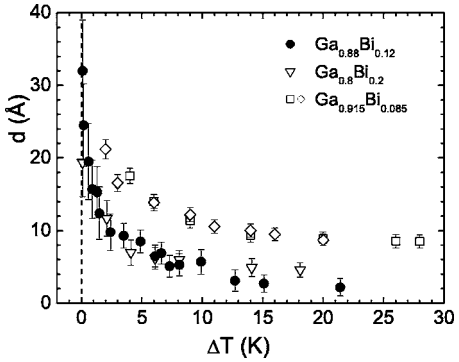

FIG. 6. Thickness of the wetting film approaching the liquid-liquid coexistence line ($\Delta T = T - T_{coex}$) for $x_{Ga}=0.915$ (□, ◇—two runs, same sample); 0.88 (●) and 0.8 (▽). Error bars represent the uncertainty of the three-phase model fit only.

results shown in Figs. 5 and 6 were obtained. The behavior of Ψ and Δ reflects the continuous increase of the thickness of a Bi-rich layer on top of the Ga-rich bulk as the complete wetting state at two-phase coexistence is reached. This is in agreement with theoretical expectations for the approach to a complete wetting state from off coexistence.[13] Moreover, it is also in agreement with independent experimental results obtained by grazing x-ray reflectivity measurements for Ga-Bi alloys.[11,12] As will be discussed quantitatively in Sec. IV C the wetting film thickness d scales in a characteristic manner with the chemical potential distance, $\Delta\mu$, to the coexistence regime.

As one enters the demixing gap in range II the formation of the wetting film is completed and the temperature of the sample drops from 258 °C to 222 °C. The composition of the wetting film at the interface is related to the composition of the bulk phase on the Bi-rich side of the coexistence curve. This is illustrated by the path B_2 to C in the phase diagram. Along this change of state Ψ and Δ decrease slightly, which can be explained by the variation of the composition of the coexisting phases according to the phase diagram. A change of the composition is accompanied by a mass density change, which may also lead to a variation of the gravity limited wetting film thickness.

The behavior of the sample temperature is remarkable: although the furnace cools down with a constant rate of 3 K/h the cooling rate of the sample temperature accelerates with the formation of the wetting film. This peculiar behavior is even visible before the sample enters the two-phase region. The reason is a change of the thermal emissivity of the sample surface. At high temperatures in range I the surface consists of the Ga-rich phase with only a microscopically thin Gibbs adsorbed Bi layer. Approaching coexistence the wetting film thickens, which is shown in Fig. 6. In principle, the dependence of the thermal emissivity on the film thickness has to be taken into account.[29] For Ga-Pb this was done by Turchanin *et al.*[30] Here we restrict ourselves to a rough estimate and consider the emissivity of pure Ga and Bi, respectively: For the perfectly flat surface of a liquid metal the emissivity $\epsilon(h\nu)$ depends on the reflectivity $R(h\nu)$: $\epsilon(h\nu) = 1 - R(h\nu)$.[31] The reflectivity of Ga and Bi can be calculated within the Drude free-electron model using the parameters of Table I. Then the product $\epsilon(h\nu)\rho(h\nu)$, where ρ is Planck's blackbody energy distribution function, is integrated for $T = 550$ K in the relevant energy range $h\nu \leqslant 1$ eV. In comparison to a true black body, the liquid Ga surface exhibits a radiative heat loss of only 8% and liquid Bi of 17%. The difference in heat loss between a pure liquid Ga sample and a pure liquid Bi sample accounts for our sample size of Ø50 mm to about 1.1 W. This is a notable amount in comparison to the power consumption of the furnace of about 10 W. Thus, at the same furnace temperature, a Ga-Bi sample covered with a Bi-rich wetting layer is a bit colder than a sample without.

Range III is the time interval where the monotectic reaction takes place. Solid Bi precipitates in the sample. In this stage four phases coexist at a tetra point: the Ga-rich liquid M in Fig. 1, the Bi-rich liquid C, solid Bi, and the vapor phase. According to Gibb's phase rule, the sample temperature approaches a constant value of 222 °C. During this change Bi crystallizes not only in the bulk but also at the surface since the Bi-rich wetting film phase is already present. In the foot print of the light beam the alloy surface may become inhomogeneous. Hence, Ψ and Δ change in an unreproducible way.

As the monotectic reaction has finished, the sample reaches range IV and the alloy surface is again a homoge-

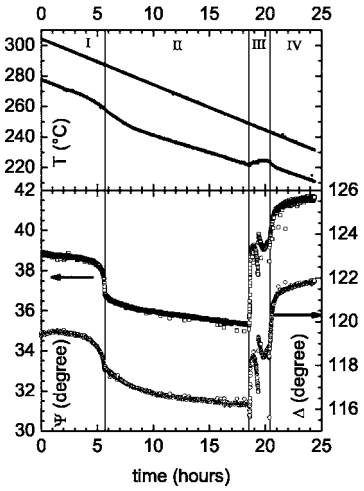

FIG. 7. Time-dependent measurements at $h\nu=2.75$ eV on continuous cooling of a $Ga_{0.8}Bi_{0.2}$ alloy: upper part—cooling curves for heater and crucible; lower part—ellipsometric angles Ψ (□) and Δ (○). On cooling along path $A_1B_1B_2CMD$ (see also Fig. 1) the following phases are exposed to the light beam at the surface of the sample: homogeneous liquid region $A_1 \rightarrow B_1$ (region I), within miscibility gap $B_1 \rightarrow B_2 \rightarrow C$ (region II), crucible temperature stays almost constant at the monotectic temperature 222 °C (region III), afterward the sample continues to cool down further on path $M \rightarrow D$ (region IV).

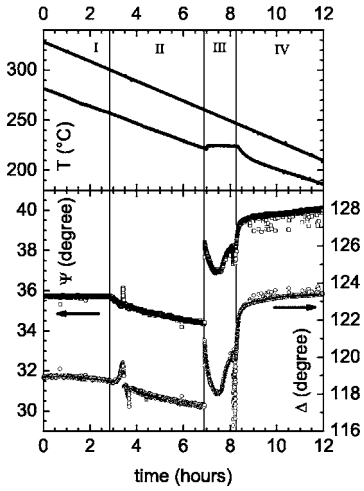

FIG. 8. Time-dependent measurements at $h\nu=2.75$ eV on continuous cooling of a $Ga_{0.57}Bi_{0.43}$ alloy: upper part—cooling curves for heater and crucible; lower part—ellipsometric angles Ψ (□) and Δ (○). Cooling proceeds in a similar way as described in Fig. 7, but along the path A_2B_2CMD. The disturbance at ~3.5 h is discussed in text.

neous Ga-rich liquid. Crystalline Bi precipitates in the bulk phase of the liquid and is not any longer visible for the ellipsometer. It is noteworthy to mention that now the sample temperature approaches the exact linear continuation of the sample temperature curve in range I. On further cooling the composition of the bulk liquid phase changes from M to D in Fig. 1. It is remarkable that Ψ and Δ now mirror the behavior in range I approaching range II. Indeed, we observe the reversal of complete wetting along the liquidus line from M to D. This part of the curve will be analyzed quantitatively in Sec. IV B. It is in agreement with x-ray reflectivity results of Huber *et al.*[11] as well as with the analysis of Auger spectra for the Ga-Pb system by Chatain and Wynblatt.[5]

These results as well as our data here were obtained as the liquidus line (path M to D, separating the homogeneous liquid Ga-rich phase from the two-phase region with a Ga-rich liquid and solid Bi) was reached on cooling from the liquid-liquid demixing regime. The Bi-rich wetting film is already present and no nucleation barrier has to be crossed. It exists along a small portion of the liquidus line. Below $T=218$ °C the liquid wetting film has vanished. To our opinion this specific path in the phase diagram should be distinguished from the approach to the liquidus line at constant composition from the homogeneous Ga-rich liquid above the monotectic point. At least for $x_{Ga} \geqslant 0.95$ second harmonic generation experiments[32] as well as ellipsometry[33] revealed the spontaneous formation of a solid Bi-rich film covering the Ga-rich bulk liquid within minutes. If there is a competition between wetting and surface freezing in close vicinity of the monotectic point is experimentally still unresolved.

Figure 8 is organized in the same way as Fig. 7: range I represents the homogeneous phase above the demixing gap (range II). The monotectic reaction is represented by range III and the temperature range below the monotectic tetra point by region IV. The cooling rate of the furnace is 10 K/h. Unlike Fig. 7, Ψ and Δ are almost constant in range I approaching the miscibility gap. Since complete wetting can only occur on the Ga-rich side of the demixing range, we have a homogeneous alloy without a wetting film until the coexistence curve is reached. In range II we observe a continuous decrease of both Ψ and Δ, which corresponds to the compositional change of the Bi-rich phase exposed to the light beam. The evolution of Ψ and Δ is interrupted by an anomaly around 3.5 h. It can be related to the onset of an oscillatory instability of the wetting film under the given thermal conditions. This phenomenon is probably analogous to a similar wetting film instability that was recently found in a Ga-Pb alloy.[30] We have studied this surprising effect in more detail[34] and it will be the subject of a forthcoming publication.[35]

Ranges III and IV in Fig. 8 are similar in comparison to those presented in Fig. 7. The monotectic reaction is accompanied by changes of Ψ and Δ, which are difficult to interpret. In range IV the same path M to D (see Fig. 1) as in the previous sample is probed. Here we observe again the thinning of a complete wetting film as we cool the sample down further.

B. Evaluation of the wetting film thickness from single-wavelength measurements approaching liquid-liquid coexistence

As was shown in Figs. 5 and 6 the wetting film thickness approaching the coexistence line from the homogeneous phase can be determined from the ellipsometric spectra in the energy range between 0.8 eV and 4.65 eV. This was achieved with the aid of the three-phase model assuming a liquid Bi-rich film and a Ga-rich bulk phase. The composi-

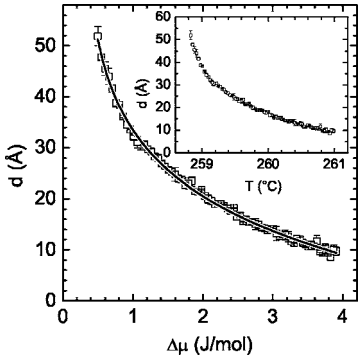

FIG. 9. x_{Ga}=0.8: thickness of the wetting film versus $\Delta\mu$ and versus T (inset) extracted from single-wavelength measurements corresponding to region I in Fig. 7. The solid line is a fit of d proportional to $\ln(\Delta\mu^{-1})$.

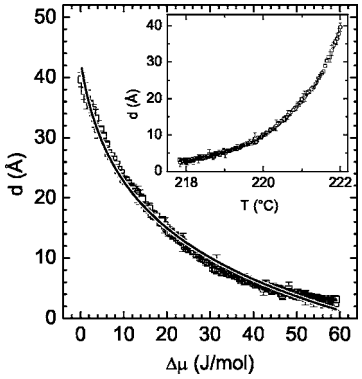

FIG. 10. x_{Ga}=0.8: thickness of the wetting film versus $\Delta\mu$ and versus T (inset) extracted from single-wavelength measurements corresponding to region IV in Fig. 7. The solid line is a fit of d proportional to $\ln(\Delta\mu^{-1})$.

tion profile is approximated as a step function and a possible concentration gradient across the film is neglected. X-ray reflectivity experiments have been interpreted in terms of a rough interface between film and substrate employing a continuous composition profile.[12] Thus, the film thicknesses accessible by ellipsometry have to be regarded as effective values.

Besides the spectra, recorded at distinct and constant temperatures, it seems to be worthwhile to evaluate the dense sequence of Ψ-Δ couples obtained on cooling in ranges I and IV. This promises a deeper insight into the variation of the wetting film thickness approaching complete wetting. The procedure has to be carried out in several steps. Since the equations of Ψ and Δ as a function of the film thickness d cannot be inverted analytically to calculate d directly, we have to apply a nonlinear least-squares-fitting routine to each dataset consisting of one pair of Ψ and Δ. An essential prerequisite is a physically meaningful choice of the complex dielectric functions for both the film, ε_{Film}, and the underlying substrate phase, ε_{Bulk}. The latter is easy to obtain since it can be calculated within the two-phase model from Ψ and Δ sufficiently far away from complete wetting. In a first iteration, we choose ε_{Film} from direct measurements of the bulk phase with a composition that can be assumed for the film. Alternatively, ε_{Film} can be calculated employing the Bruggeman approximation (EMA). In the next step, we fit for each pair of Ψ and Δ (in ranges I and IV, Fig. 7) the corresponding film thickness and obtain a dataset of d of zeroth order as a function of the temperature T. In a third step, a flexible function with only a few parameters is chosen to achieve a phenomenological description of $d(T)$. Both full datasets $\Psi(T)$ and $\Delta(T)$ are then (fourth step) fitted simultaneously to optimize the parameters for the functional description of $d(T)$ as well as ε_{Bulk} and ε_{Film}. The agreement between fits and datasets was within the scattering of the experimental values. It turned out that ε_{Bulk} consistently approaches a stable value measured about 10 K away from the two-phase regime. However, for such an optimal fit of $\Psi(T)$ and $\Delta(T)$ we have to allow some variation for ε_{Film} although in close borders. This is not surprising since deviations from the bulk values might occur for a thin film phase with a thickness between one monolayer to about 50 Å. With the new values of ε_{Bulk} and ε_{Film}, we fitted again the film thickness d for each Ψ-Δ pair to obtain the final relation of d with temperature. The result is presented in the inset of Fig. 9 for the approach to complete wetting from above the demixing gap (range I in Fig. 7). The result for complete wetting below the monotectic temperature (range IV in Fig. 7) is presented in the inset of Fig. 10. The numerical details for the treatise described above are presented in the Appendix.

For case I it turned out that the absolute value of the film thickness depends very sensitively on the choice of ε_{Film}. The absolute accuracy lies within a factor of two. The reason for this is the small compositional difference between bulk phase (x_{Bulk}=0.8) and film phase ($x_{Film}\approx 0.6$) and, consequently, a small contrast between ε_{Bulk} and ε_{Film}. However, the functional form of $d(T)$ is not affected by the choice of ε_{Film} and $d(T)$ can be calibrated with the help of the three-phase fits of the spectra (Fig. 6). For case IV the compositional difference between bulk phase (x_{Bulk}=0.9) and film phase ($x_{Film}\approx 0.4$) and, thus, the contrast between ε_{Bulk} and ε_{Film} is much more pronounced. This leads to a smaller absolute error (about 20%) for the film thickness.

C. Scaling of the wetting film thickness growth

The approaches toward the demixing gap from the homogeneous phase (A_1 to B_1 in Fig. 1) as well as the route along the liquidus line below the monotectic temperature (M to D in Fig. 1) represent two special paths toward and away from complete wetting. Along these paths the wetting film is not a stable bulk phase and its formation costs a certain amount of free energy. These energetic costs are provided by a thickness-dependent contribution arising from the repulsion of the interfaces of the wetting film. The latter depends on the specific intermolecular interactions in the film and between film and the adjoining bulk phases. The energetic distance between the actual state of the system and the state at liquid-liquid coexistence is usually measured with the help of the quantity $\Delta\mu$, which is related to the chemical potentials of both components: μ_{Bi} and μ_{Ga}. Depending on the nature of the intermolecular interactions, different dependences of the wetting film thickness d with $\Delta\mu$ are

predicted:[36] for algebraically decaying, i.e., long range interactions like van der Waals forces, d should be proportional to $\Delta\mu^{-1/3}$. In the case of short range interactions, like the exponentially decaying screened Coulomb potential in a liquid metal we expect d to be proportional to $\ln(\Delta\mu^{-1})$.

To have access to the quantity $\Delta\mu$ we assume that the molar free enthalpy of the mixture, $G_m(x,T)$, can be expressed as an analytical function in the relevant composition and temperature range. As usual the equilibrium compositions of the coexisting phases α and β are defined by a common tangent construction,[37] which ensures for the chemical potentials at the coexistence of the phases α and β: $\mu_{\mathrm{Ga}}(\alpha)=\mu_{\mathrm{Ga}}(\beta)$ and $\mu_{\mathrm{Bi}}(\alpha)=\mu_{\mathrm{Bi}}(\beta)$. The free enthalpy as a function of composition and temperature is available in the literature.[12] Huber *et al.* fitted the coefficients of Redlich-Kister polynomials in the framework of an extended regular solution model to describe quantitatively the thermodynamics of the mixture and the liquid-liquid demixing phase line in the interesting temperature and composition range.[38] Once $G_m(x,T)$ is known the μ_i follow by the method of intercepts ($x=x_{\mathrm{Ga}}$): $\mu_{\mathrm{Ga}}(x,T)=G_m(x,T)+(1-x)[\partial G_m(x,T)/\partial x]_T$ and $\mu_{\mathrm{Bi}}(x,T)=G_m(x,T)-x[\partial G_m(x,T)/\partial x]_T$. According to Dietrich and Schick, $\Delta\mu$ is calculated at constant temperature in a plane spanned by the independent coordinates $a=(\mu_{\mathrm{Bi}}+\mu_{\mathrm{Ga}})$ and $b=(\mu_{\mathrm{Bi}}-\mu_{\mathrm{Ga}})$.[13] The sum of the chemical potentials can be related to the pressure of the system, whereas the difference can be regarded as a measure for the composition. $\Delta\mu$ is then the absolute value of a vector connecting two points in that plane, i.e., $[\Delta\mu]^2=[\Delta a]^2+[\Delta b]^2$. The situation is nicely illustrated for our present system in Fig. 2 of Ref. 12.

For case I in Fig. 7, $\Delta\mu$ is calculated along path A_1 to B_1, i.e., it measures the distance between $x_{\mathrm{Ga}}=0.8$ and $x_{\mathrm{Ga}}=x_{\mathrm{Ga,coex}}$ in terms of the chemical potentials along the Ga-rich branch of the coexistence curve ranging from the critical point down to B_1. For case IV, $x_{\mathrm{Ga}}=x_{\mathrm{Ga,sl}}$ is not constant, instead it is given as the composition along the liquidus line from M to D. The relevant composition $x_{\mathrm{Ga,coex}}$ in this case is measured along the Ga-rich branch of the metastable extension of the liquid-liquid demixing curve below M. This last line is shown in Fig. 1 as a dashed line.

In Fig. 9 and Fig. 10 we present the evolution of the film thickness d as a function of $\Delta\mu$ for case I and for case IV, respectively. For clarity the insets in the figures show the film thickness as a function of temperature. Included in the figures are fits according to $d=\xi\ln[\Phi/(\Delta\mu-\delta_0)]$ which is the proposed logarithmic divergence of the film thickness assuming short range interactions. ξ is the bulk correlation length, Φ is a measure for the strength of the effective surface potential, and δ_0 accounts for the experimental uncertainty of the exact location of the demixing temperature at the given mole fraction. In Fig. 11 we have rescaled the information of Fig. 6 for the sample with $x_{\mathrm{Ga}}=0.88$ and show d as a function of $\Delta\mu$. It has to be emphasized that unlike Figs. 9 and 10, each film thickness value was determined at constant temperature from a full spectrum employing the three-phase model. For this composition x-ray reflectivity experiments of Huber *et al.* allow an independent comparison of the wetting film thickness.[11,12] Unfortunately, from

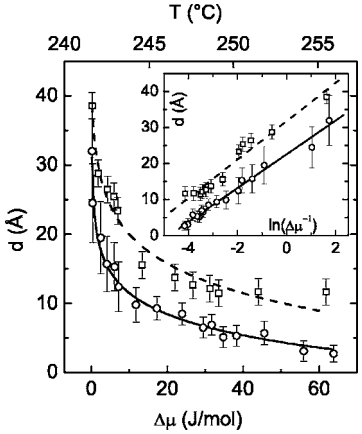

FIG. 11. $x_{\mathrm{Ga}}=0.88$: thickness of the wetting film versus $\Delta\mu$ extracted from ellipsometric spectra in the homogeneous phase region above the demixing gap. ○, this work; solid line, fit according to $d\propto\ln(\Delta\mu^{-1})$; □, data of Huber *et al.* as scanned from their Fig. 3(b) in Ref. 11 (error bars correspond to symbol size); dashed line, fit according to $d\propto\ln(\Delta\mu^{-1})$. Inset: Same data presented as d versus $\ln(\Delta\mu^{-1})$.

these two publications it is not possible to understand how the authors calculated the $\Delta\mu$ scale. Thus, the film thickness values were scanned from their d vs T diagram in Fig. 3(b) of Ref. 11. In a second step, the chemical potentials $\mu_{\mathrm{Ga}}(x_{\mathrm{Ga}}=0.88,T)$, $\mu_{\mathrm{Bi}}(x_{\mathrm{Ga}}=0.88,T)$ and, finally, $\Delta\mu(T)$ were determined as described above. The x-ray reflectivity results are included in Fig. 11 and the error bars reflect the symbol size in the original publication. In the inset the film thickness d is shown in a linearized form versus $\ln(\Delta\mu^{-1})$.

We have summarized the fitting results in Table II. First of all, the temperature correction parameters δ_0 correspond in all cases to a temperature uncertainty not bigger than 0.2 K. Thus, it needs no further consideration, since it is significantly smaller than the temperature error arising from the experimental determination of T and the uncertainty of the knowledge of the phase diagram. Besides this the following observations are worth noting.

In the experiments shown in Fig. 11 ($x_{\mathrm{Ga}}=0.88$) we find the correlation lengths ξ in the range of 4 to 7 Å and potentials Φ of the order of 100 to 250 J/mol. The discrepancy is only seemingly, since Φ strongly depends on the choice of the data points included in the fit and on the error of the ellipsometric determination of the film thickness. Omitting the last two data points at the upper end of the $\Delta\mu$ scale and allowing for an error of the ellipsometric d values of about 3 Å, we obtain almost agreement for ξ and Φ between x-ray reflectivity and ellipsometry. This also means that on the basis of the present ellipsometry and x-ray data, ξ and Φ should be interpreted carefully.

For the single-wavelength experiment performed on slow cooling of the sample ($x_{\mathrm{Ga}}=0.8$) we obtain a correlation length $\xi=15$ Å, which is a factor 2 or 3 higher than in the previous case and a potential $\Phi=7$ J/mol, which is a factor of 20 to 30 lower. Since the composition of this sample is closer to the critical point at $x_{\mathrm{Ga}}=0.7$, an increase of the correlation length is expected. In addition, the composition of the bulk phase and the wetting film is not as different as in

TABLE II. Fitting parameters for the film thickness d as a function of $\Delta\mu$ shown in Figs. 9–11.

Fig. No.	x_{Ga}	T range (°C)	ξ (Å)	Φ (J mol^{-1})	δ_0 (J mol^{-1})	Remarks
9	0.8	261→258.8	15	7	0.3	I, Fig. 7 (3 K/h)
10	Along liquidus line below monotectic point	222→218	14	69	−3	IV, Fig. 7 (3 K/h)
	Along liquidus line below monotectic point	222→218	21	78	−0.3	IV, Fig. 8 (10 K/h)
11	0.88	255→242	4.4	135	0.06	• in Fig. 6
11	0.88	255→242	6.3	250	−0.3	from Ref. 11

the case of $x_{Ga}=0.88$ and, therefore, a smaller potential parameter is reasonable. However, the situation is not yet clear, since the small but finite cooling rate might possibly influence the results due to the fact that equilibration can be extremely slow.

Two experiments concerning complete wetting below the demixing gap at 222 °C $\geqslant T \geqslant$ 218 °C are included in Table II (case IV in Figs. 7 and 8). The potential parameters are similar and lie between 70 and 80 J/mol but the correlation length accounts for 14 Å and 21 Å, respectively. The only difference in both experiments is a cooling rate of 3 K/h in the former and of 10 K/h in the latter case. It is known that the kinetics of wetting phenomena can be pretty slow and in so far it is not clear if we can exclude an effect of the cooling rate on the results. This problem and a refinement of the simple three-phase model for the interpretation of our spectra have to be considered in future experiments.

Last but not least, even though ξ and Φ differ to some extent in the experiments shown here, it has to be pointed out that fits according to $d \propto \Delta\mu^{-1/3}$ never gave physically significant results. This means that the functional form of d with $\Delta\mu$ proposed for short range interactions is probably correct, at least in the composition and temperature range of our experiments. The expected[13] crossover to long range van der Waals behavior approaching complete wetting is not yet discernable. It occurs possibly at a larger wetting film thickness in comparison to those observed in this study. The wetting film thickness is also dependent on the height of the Ga-rich subphase so that the crossover might become visible after changing the sample geometry and, thus, the subphase height.

V. CONCLUSIONS

Single-wavelength and spectroscopic ellipsometry are useful tools to probe bulk and surface properties of metallic alloys. They are relatively inexpensive and complementary to microscopic probes like x-ray reflectivity or grazing x-ray diffraction. It was shown that the optical properties of liquid Ga as well as liquid Bi can be quantitatively described using the classical Drude model for free electrons. In addition, the spectra of liquid homogeneous alloys of Ga and Bi are quantitatively modeled in the framework of a Bruggeman effective medium approximation. This was not *a priori* expected since effective medium models have been developed for inhomogeneous composites consisting of domains of the pure components big enough to maintain their bulk optical properties. Perhaps this result can be generalized for alloys with a tendency for demixing in their phase diagram. On the other hand, it is highly questionable if such an EMA approach works for compound forming alloys.

The main objective of the present investigations was focused on the wetting film thickness as the complete wetting state at liquid-liquid coexistence is approached via different routes in a binary fluid alloy. It is surprising that under our present experimental conditions the complete wetting state at liquid-liquid coexistence is not stable *ad infinitum*. An interplay between heat influx from the furnace and—due to a wetting film thickness dependent emissivity of the sample—a varying heat loss leads to oscillatory instabilities with a period of several hours.

Single-wavelength as well as spectroscopic ellipsometry clearly revealed the wetting film thickness divergence approaching or departing liquid-liquid coexistence. It increases from the microscopic Gibbs adsorbed layer to about 30 Å to 50 Å in close vicinity to coexistence. While the absolute value of the film thickness can be calibrated by ellipsometric spectra at constant temperature, the single-wavelength measurements on continuous cooling elucidate how the wetting film scales with the distance to complete wetting at coexistence. In all experiments we found clear evidence for the logarithmic divergence, typical for short range wetting. The parameters describing the scaling properties are the bulk correlation length ξ and the effective interface potential Φ. Depending how close the exact path toward complete wetting is located at the bulk critical point ξ varies between 5 Å and 15 Å. The relatively broad bandwidth of Φ between 7 J/mol and 250 J/mol is not yet easy to explain. Different compositions of bulk and film may contribute to our result, but at present it is not clear if this is the only explanation. A deeper interpretation may be possible when the influence of the cooling rate can be estimated.

ACKNOWLEDGMENTS

This work was supported through the Centre for Functional Nanostructures of the Deutsche Forschungsgemeinschaft (DFG-CFN: www.cfn.uni-karlsruhe.de). We thank P.

Huber and P. Pershan (Harvard University) for submitting their results on the phase diagram calculations prior to publication.

APPENDIX

Case I

For the simultaneous fits of the $\Psi(T)$ data set and $\Delta(T)$ data set at a constant energy of 2.75 eV, we obtained for an optimal phenomenological description of the film thickness d (in Å) as a function of T (in °C)

$$d(T) = 1.47 + 37.7 \exp\left[-\frac{T-258.8}{1.3}\right] + 16.57 \exp\left[-\frac{T-258.8}{0.138}\right]$$

and the following values for the complex dielectric functions of substrate phase and film phase

$$\varepsilon_{Bulk} = \varepsilon_{1,Bulk} - i\varepsilon_{2,Bulk} = -17.79 - i10.68,$$

$$\varepsilon_{Film} = \varepsilon_{1,Film} - i\varepsilon_{2,Film} = -14.38 - i13.25.$$

Fitting each Ψ-Δ pair with these $\varepsilon_{\mathrm{Bulk}}$ and $\varepsilon_{\mathrm{Film}}$ yields $d(T)$ as presented in the inset of Fig. 9.

Case IV

For the simultaneous fits of the $\Psi(T)$ data set and $\Delta(T)$ data set at a constant energy of 2.75 eV, we obtained for an optimal phenomenological description of the film thickness d (in Å) as a function of T (in °C)

$$d(T) = \exp(1004 - 9.746T + 2.361 \times 10^{-2}T^2)$$

and the following values for the complex dielectric functions of substrate phase and film phase

$$\varepsilon_{Bulk} = \varepsilon_{1,Bulk} - i\varepsilon_{2,Bulk} = -22.38 - i7.42,$$

$$\varepsilon_{Film} = \varepsilon_{1,Film} - i\varepsilon_{2,Film} = -14.11 - i13.19.$$

Fitting each Ψ-Δ pair with these $\varepsilon_{\mathrm{Bulk}}$ and $\varepsilon_{\mathrm{Film}}$ yields $d(T)$ as presented in the inset of Fig. 10.

*Corresponding author. Electronic address: Nattland@ipc.uka.de

[1] S. Dietrich, in *Phase Transitions and Critical Phenomena*, edited by C. Domb and J. Lebowitz (Academic Press, London, 1987), Vol. 12.
[2] M. Schick, in *Liquids at Interfaces, Les Houches Session XLVIII*, edited by J. Charvolin, J. F. Joanny, and J. Zinn-Justin (North-Holland, Amsterdam, 1990).
[3] D. Bonn and D. Ross, Rep. Prog. Phys. **64**, 1085 (2001).
[4] D. Nattland, P. D. Poh, S. C. Müller, and W. Freyland, J. Phys.: Condens. Matter **7**, L457 (1995); D. Nattland, S. C. Müller, P. D. Poh, and W. Freyland, J. Non-Cryst. Solids **205–207**, 772 (1996); D. Nattland, H. Chadli, C. A. Zell, S. C. Müller, B. v. Blanckenhagen, and W. Freyland, Ber. Bunsenges. Phys. Chem. **102**, 1151 (1998).
[5] D. Chatain and P. Wynblatt, Surf. Sci. **345**, 85 (1996).
[6] B. Predel, Z. Phys. Chem., Neue Folge **24**, 206 (1960).
[7] R. A. Khairulin, S. V. Stankus, and A. L. Sorokin, J. Neurosci. Res. **297**, 120 (2002).
[8] A. H. Ayyad and W. Freyland, Surf. Sci. **506**, 1 (2002).
[9] C. Serre, P. Wynblatt, and D. Chatain, Surf. Sci. **415**, 336 (1998).
[10] W. Freyland, A. H. Ayyad, and I. Mechdiev, J. Phys.: Condens. Matter **15**, S151 (2003).
[11] P. Huber, O. G. Shpyrko, P. S. Pershan, B. M. Ocko, E. DiMasi, and M. Deutsch, Phys. Rev. Lett. **89**, 035502 (2002).
[12] P. Huber, O. Shpyrko, P. S. Pershan, B. Ocko, E. DiMasi, and M. Deutsch, Phys. Rev. B **68**, 085409 (2003).
[13] S. Dietrich and M. Schick, Surf. Sci. **382**, 178 (1997).
[14] R. M. A. Azzam and N. M. Bashara, *Ellipsometry and Polarized Light* (North-Holland, Amsterdam, 1987).
[15] S. N. Jasperson and S. E. Schnatterly, Rev. Sci. Instrum. **40**, 761 (1969).
[16] B. Drevillon, N. Y. Parey, M. Stchakovsky, R. Benferhat, Y. Josserand, and B. Schlayen, Proc. SPIE **1188**, 174 (1990).
[17] B. C. Allen, in *Liquid Metals Chemistry and Physics*, edited by S. Z. Beer (Marcel Dekker, New York, 1972).
[18] G. Indlekofer, P. Oelhafen, and H. J. Günterodt, in *Phys. Chem. Prop. Thin Met. Overlayers Alloy Surf.*, edited by D. M. Zehner and D. W. Goodman, MRS Symposia Proceedings No. 83 (Materials Research Society, Pittsburgh, 1987), p. 75.
[19] D. E. Aspnes, in *Handbook of Optical Constants of Solids*, edited by E. D. Palik (Academic Press, Boston, 1985).
[20] N. R. Comins, Philos. Mag. **25**, 817 (1972).
[21] R. S. Teshev and A. A. Shebzukhov, Opt. Spectrosc. **65**, 693 (1989).
[22] N. V. Smith, Adv. Phys. **16**, 629 (1967).
[23] T. Inagaki, E. T. Arakawa, A. R. Cathers, and K. A. Glastad, Phys. Rev. B **25**, 6130 (1982).
[24] See EPAPS Document No. E-PRBMDO-72-060528 for two tables of the complex dielectric functions of Ga and Bi at various temperatures. This documents can be reached via a direct link in the online article's HTML reference section or via the EPAPS homepage (http://www.aip.org/pubservs/epaps.html).
[25] See e.g., P. Grosse, *Freie Elektronen in Festkörpern* (Springer, Berlin, 1979).
[26] D. J. Steinberg, Metall. Trans. **5**, 1341 (1974).
[27] N. E. Cusack and J. E. Enderby, Proc. Phys. Soc. London **75**, 395 (1960).
[28] R. Tsekov and W. Freyland, J. Phys.: Condens. Matter **15**, 6155 (2003).
[29] P. Pigeat, D. Rouxel, and B. Weber, Phys. Rev. B **57**, 9293 (1998).
[30] A. Turchanin, R. Tsekov, and W. Freyland, J. Chem. Phys. **120**, 11171 (2004).
[31] N. M. Ravindra *et al.*, Int. J. Thermophys. **22**, 1593 (2001).
[32] A. Turchanin, W. Freyland, and D. Nattland, Phys. Chem. Chem. Phys. **4**, 647 (2002).
[33] K. Bartel, A. Kumar, D. Nattland, and W. Freyland (unpublished).
[34] S. Dogel, Ph.D. thesis, University of Karlsruhe, 2004, Univer-

sitätsverlag Karlsruhe, ISBN 3-937300-08-2, www.uvka.de.
[35] S. Dogel, W. Freyland, D. Nattland, R. Tsekov, and A. Turchanin (unpublished).
[36] See e.g., the discussion of Eq. (3.16) in Ref. 1.
[37] See e.g., C. H. P. Lupis, *Chemical Thermodynamics of Materials* (North-Holland, New York, 1983).
[38] A misprint in Ref. 12 has to be noted: the first coefficient of the zeroth Redlich-Kister polynomial must read 8000 instead of 80 000.